IL NUOVO CIMENTO Vol. 29 C, N. 1 Gennaio-Febbraio 2006
DOI 10.1393/ncc/i2005-10220-4

# Mediterranean summer temperature and winter precipitation, large-scale dynamics, trends(*)

E. Xoplaki(1)(**), J. Luterbacher(1) and J. F. González-Rouco(2)

(1) *Istitute of Geography and NCCR Climate, University of Bern Bern, Switzerland*

(2) *Departamento de Astrofísica y CC. de la Atmósfera, Universidad Complutense de Madrid Madrid, Spain*

(ricevuto l'1 Settembre 2005)

**Summary.** — In this contribution we summarize results on the large-scale influence of the atmospheric circulation at several tropospheric levels and Mediterranean SSTs on wet season precipitation and warm season temperature across the Mediterranean area covering the last few decades. Three large-scale predictor fields (300 hPa geopotential height, 700–1000 hPa thickness and SSTs) account for more than 50% of the total summer temperature variability over the Mediterranean area. The positive phase of the first most important canonical mode is associated with blocking conditions, subsidence and stability related to warm Mediterranean summers. The second CCA mode shows an east-west dipole of the Mediterranean summer air temperature connected by a combination of a trough as well as an extended ridge over the western and eastern parts of the Mediterranean, respectively. It is mainly the first mode which is responsible for the significant 0.4°C warming over the last 50 years of the twentieth century. In the context of the last 500 years it comes apparent that the hot summers of the decade 1994-2003 seem to be unprecedented. The hottest larger Mediterranean summer over the last half millennium was in 2003, in agreement with findings from the whole of Europe. It is found that around 30% of the total Mediterranean October to March precipitation variability can be accounted for by the combination of four large-scale geopotential height fields and sea level pressure. Results show that the North Atlantic Oscillation (NAO) seems to play an important role in interannual to centennial low frequency variability of wet season precipitation over the studied area. In the western and northern part, the correlation between precipitation and the NAO is negative, whereas for the southeastern part mostly positive correlations have been found. The analysis further reveals that since the mid-nineteenth century precipitation steadily increased with a maximum in the 1960s and decreased since then. The second half of the twentieth century shows a general downward trend of 2.2 mm/month/decade.

PACS 92.60.Ry – Climatology.
PACS 92.70.Gt – Climate dynamics.
PACS 92.60.Bh – General circulation.
PACS 01.30.Cc – Conference proceedings.

(*) Paper presented at the Workshop on "Historical Reconstruction of Climate Variability and Change in Mediterranean Regions", Bologna, October 5-6, 2004.
(**) E-mail: xoplaki@giub.unibe.ch

## 1. – Introduction

The understanding and knowledge of spatio-temporal patterns of climate change for the last centuries remains a major task in assessing the degree to which the twentieth century was unusual in view against a background of pre-industrial climate variability. Further, there is an ongoing discussion on the vulnerability of ecosystems due to global change and increasing drought risk. The Mediterranean is a climate-sensitive and stressed region by limited water resources and extremes of summer heat assisting the creation or exacerbation of existing sociopolitical tensions. In this short contribution, we will compile results from [33-35] dealing with the large-scale atmospheric influence and SST on winter Mediterranean precipitation and summer temperature, respectively and discuss trends for the second part of the twentieth century. In order to address the current changes in summer Mediterranean temperature in a longer time context, we present reconstructed averaged time series over the larger Mediterranean land areas (extracted from the European temperature reconstructions by [17]). We discuss the evolution of summer mean temperatures for half a millennium in the context of estimated uncertainties and emphasizing trends and extremes.

## 2. – Data and methods

The following data sets have been used: (1) Gridded ($2.5° \times 2.5°$ latitude-longitude resolution) SLP data and geopotential heights at different levels (1000 hPa, 850 hPa, 700 hPa, 500 hPa and 300 hPa) were taken from the NCEP/NCAR reanalysis data sets [13, 14]. The monthly SST data were taken from the Global Sea Ice Surface Temperature, version 2.3b (GISST2; spatial resolution is $1° \times 1°$ latitude-longitude) dataset [25]). (2) Monthly station series of air temperature and precipitation for the area 25° N-48° N and 10° W-45° E including 30 countries along or close to the Mediterranean Sea were collected and digitized. The data were obtained mainly from the various National Meteorological services or other official institutions. For countries that did not provide any data, the GHCN (Global Historical Climatology Network) version 2 air temperature and version 2b precipitation data have been used, which are extensively quality controlled [30, 23, 24]. We follow the approach presented in [32] assessing the connection between large-scale dynamics and Mediterranean surface air temperature and precipitation. Specifically, a downscaling model is calibrated using Canonical Correlation Analysis (CCA) in the Empirical Orthogonal Function (EOF) space and subsequently this model is validated by means of cross-validation. For a detailed description of the methodology the reader is referred to [33, 34]; for an extended discussion about EOF, CCA and cross-validation see [1, 19, 31] and [29]. Before performing the CCA, the original data were projected onto their EOFs retaining only a limited number of them, accounting for most of the total variance in the datasets. As a preliminary step to the calculation of EOFs, the annual cycle was removed from all station and grid point time series. The gridded predictor data were then weighted to account for the latitudinal variation of the grid area [20, 16]. A further step to ensure the stationarity of the variables was to detrend the time series by a standard linear least square fit method. [4, 17] presented gridded (60 km $\times$60 km resolution) seasonal surface air temperature reconstructions for the European continent. They are based on multivariate statistical climate fields reconstruction (CFR) approaches (*e.g.* [12, 17, 36]. CFR seeks to reconstruct a large-scale field of surface air temperature using a spatial network of proxy indicators, performing a multivariate calibration of the large-scale information in the proxy data network (documentary evidence,

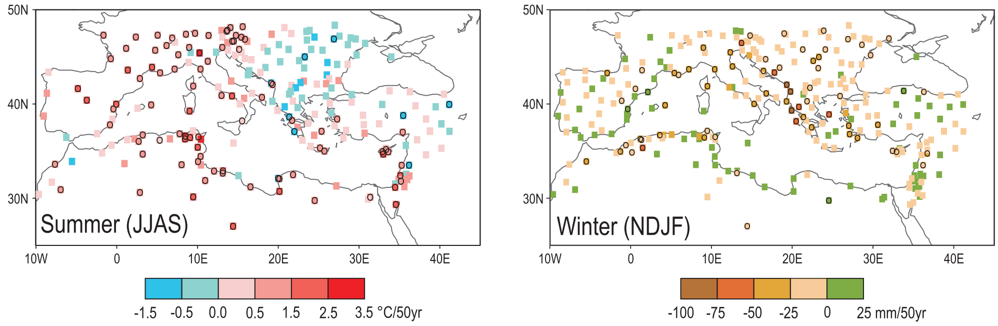


Fig. 1. – Right: linear trends of wet season station precipitation (mm/50 y) and left: summer surface air temperatures (°C/50 y) for the 1950-1999 period. Stations with a significant trend (90% confidence level, based on the Mann-Kendall test) are encircled (from Xoplaki, 2002).

natural proxies) against the gridded land-based data of the Climatic Research Unit. Here we used the reconstructed European land temperature from [17], extracting the larger Mediterranean area from 35° N-47° N and 10° W-40° E, though re-calculating 2 sigma uncertainties for averaged summer temperature back to 1500.

## 3. – Results and discussion

**3**˙1. *Mediterranean summer temperature and wet season precipitation trends*. – Reference [8] analyzed the surface air temperature variability and trends over the larger Mediterranean land-area for the twentieth century based on gridded data of [21]. He found a significant annual warming trend of 0.75 °C, mostly from contributions in the early and late decades of the century. The structure of climate series can differ considerably across regions and seasons showing variability at a range of scales in response to changes in the direct radiative forcing and variations in internal modes of the climate system [22, 9, 8]. Figure 1 (left) presents the linear trends of summer surface air temperatures (°C/50 y) for the period 1950-1999. It also shows the stations, which experienced a significant trend [32]. A clear east-west differentiation in Mediterranean summer air temperature trends is visible. Cooling, though mostly not significant, was experienced over the Balkans, and parts of the eastern basin. In the other areas, there is a significant warming trend of up to 3 °C/50 y. However, the warming in these regions did not occur in a steady or monotonic fashion. Over most of western Mediterranean for instance, it has been mainly registered in two phases: from the mid-1920s to 1950 (not shown) and from the mid-1970s onwards (*e.g.* [2, 3, 7]).

Recent studies revealed that the twentieth century was characterized by significant precipitation trends at different time and space scales (*e.g.* [22,6,8] found negative winter precipitation trends over the larger Mediterranean land-area for the twentieth century). Using the same data, [10] showed for the last three decades some rainfall increases in autumn (western Iberia and southern Turkey), but dominating decreases in winter and spring. A glance at the Mediterranean regional precipitation trends for the 1950-1999 period reveals a more detailed picture of the general findings. Subregional variability is high, particularly in areas with contrasted topography near coastland where also significant trend in variability and monthly totals have been observed (*e.g.* [27, 28]). The evaluation of regional data series (fig. 1, right) indicate that trends in many regions

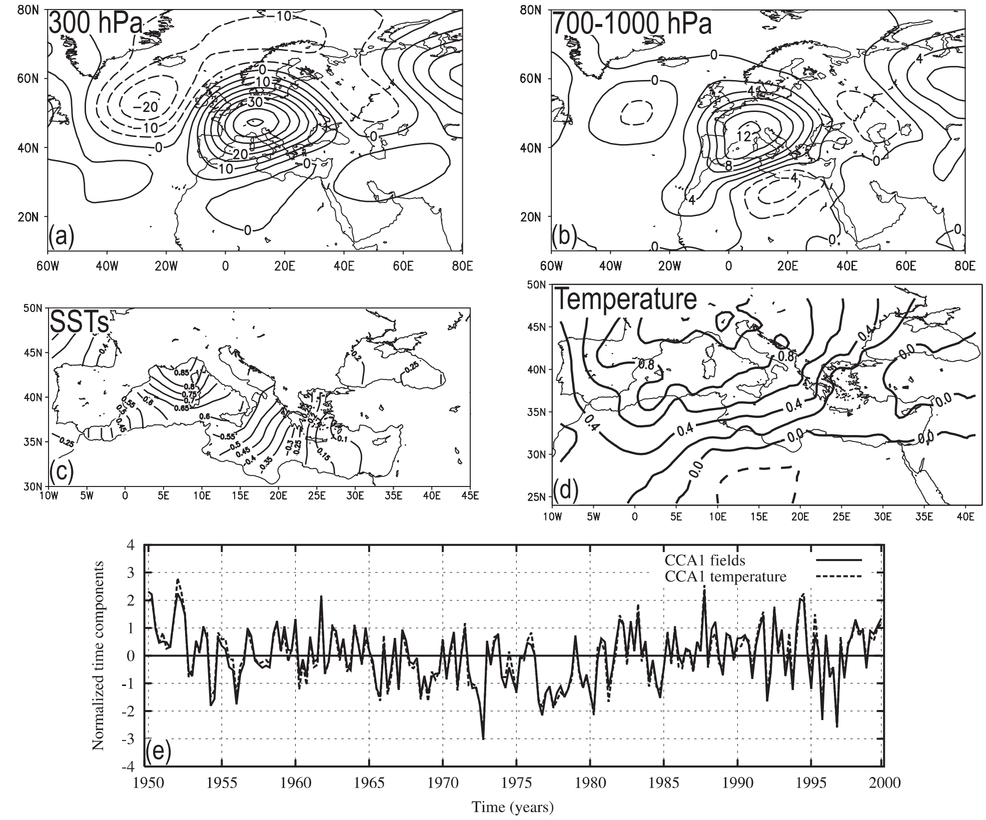


Fig. 2. – Canonical spatial patterns of the first CCA. The canonical correlation patterns reflect the typical strength of the signal, with a) 300 hPa; b) 700–1000 hPa; c) SST; d) summer air temperature anomalies in °C; e) normalised time components of CCA1 (from Xoplaki *et al.*, 2003b).

are not statistically significant in view of the large variability [32]. However, significant decreases are prevalent in western, central and the eastern Mediterranean.

**3**˙2. *Mediterranean summer temperature*. – In order to study the interannual covariability between the Mediterranean summer air temperature and the combined large-scale circulation at different levels, thickness and SST fields during the period 1950-1999, we have performed multicomponent CCA experiments including three predictor fields for summer temperature. The 300 hPa geopotential height pattern for the first CCA mode (fig. 2) reveals a dipole configuration in the North Atlantic. A strong center with positive anomalies is located over central Europe; an area of negative anomalies presents higher values south of Iceland and surrounding northward the positive anomalies extends up to the western Ural Mountains and the northern Caspian Sea. The geopotential height and thickness fields show a similar configuration indicating higher (lower) temperatures in the high (low) pressure regions. SSTs and surface temperatures reveal higher values in the northwestern part of the Mediterranean under the high-pressure region. This dynamic configuration strengthens the zonal flow over northern Europe and easterly-northeasterly flow over the Mediterranean. The increased stability leads to clear sky conditions and

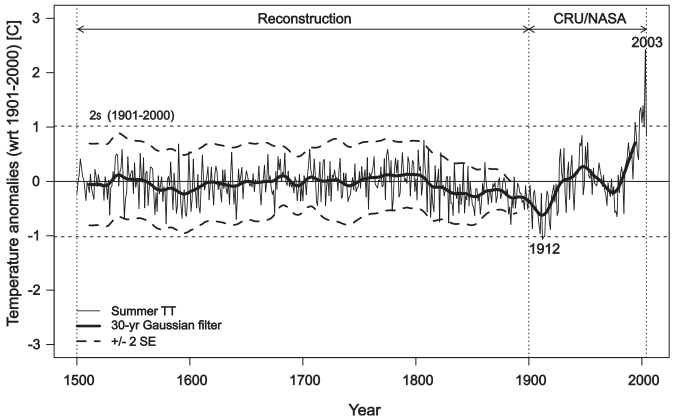


Fig. 3. – Summer mean averaged Mediterranean land temperature anomalies (with respect to 1901-2000) time series from 1500-2004 defined as the mean over the land-area 10 °W-40 °E; 35 °N-47 °N (thin black line). The values for the period 1500 to 1900 are reconstructions; data from 1901-2000 stem from the Climatic Research Unit, Norwich, U.K. The post-2000 data stem from GISS NASA surface temperature analysis given on a $1^\circ \times 1^\circ$ resolution; `http://www.giss.nasa.gov/data/update/gistemp/`). The thick line is a 30-year Gaussian low-pass filtered time series. The dashed lines show the ±2 SEs of the filtered reconstructions on either side of the low-pass filtered values. The horizontal line is the 2 standard deviation line of the period 1901-2000. The warmest and the coolest summers are denoted (from Luterbacher *et al.*, 2004).

maximum insolation in the area. The authors in [33] have shown that precipitation presents positive correlation values with the negative geopotential height regions and negative values with the positive geopotential height areas supporting the presence of clear skies and stability in the warm highs. Thus, the radiative *bonus* favoured by the dynamical configuration could be the main factor allowing for the higher temperatures in the warm high-pressure regions. The SSTs anomaly structure follows that of the atmospheric anomalies. Since the atmospheric structure dominates over a much larger area than the sea anomaly pattern and also over the whole troposphere, we suggest that the atmosphere seems to be the forcing agent for the ocean in this CCA mode [34]. This CCA mode is related to warm summers, blocking conditions, subsidence and stability over the Mediterranean. Further, warm summers can be attributed to a warm lower troposphere as shown by thickness variables and positive Mediterranean SSTs. Figure 2e shows the first pair of canonical series indicating variability from monthly to interdecadal scales. The late 1960s and 1970s present a tendency to a higher frequency of cooler. The 1950s and 1990s indicate however a tendency to warmer summers. This forms the interdecadal variability in this canonical mode showing a negative trend since the beginning of the period to the late 1970s and a positive trend since then to the end of the twentieth century. The correlation between this series and the spatial average of summer temperature is 0.76 (significant at the 95% level). Therefore, in view of these results we suggest that the long-term trends in Mediterranean summer temperatures through the twentieth century are inherently related to the variation of the first canonical mode [34].

**3**·3. *500-year Mediterranean summer temperature*. – Figure 3 presents the averaged summer Mediterranean land temperature anomalies (with respect to 1901-2000) time series from 1500-2004 defined as the mean over the land-area 10° W-40° E; 35° N-47° N and associated uncertainties calculated from unresolved variance within the twentieth century calibration period [17]. Results indicate decadal to interdecadal summer temperature variability on which shorter period quasi-oscillatory behavior is superimposed. Averaged Mediterranean summer temperatures from 1500 to around 1800 were not distinctly cooler compared to the twentieth century. The uncertainties are of the order of 0.8 °C for this period. There is summer cooling trend of around half a degree until the beginning of the twentieth century with 1912 being the coldest summer in the entire series. A glance at the spatial distribution of this summer reveals largest negative departures (up to 4 °C) over the southern France, the Iberian Peninsula and northwestern Africa (not shown). The twentieth century is characterized by a strong increase in summer temperature until around the 1950s followed by a cooling trend till the mid 1970s. Subsequently an exceptionally strong, unprecedented warming is observed which featured very likely the hottest summer decade 1994-2003, exceeding 2 standard deviations of the twentieth century. As for the whole of Europe, the summer of 2003 was by far the hottest over the last centuries. The spatial distribution for summer 2003 indicates overall strong positive deviations with maximum values over the central northern Mediterranean, France and Switzerland (not shown). The 2003 heat wave caused more than 30000 deaths, mainly in France, Italy and Germany. Further, fires destroyed huge areas of forests, mainly in Portugal and Spain.

**3**˙4. *Mediterranean wet season precipitation.* – The first CCA pair (fig. 4) between the Mediterranean wet season precipitation and the combined large-scale circulation at different levels during the period 1949-1999 accounts for 16.4% of the wet season precipitation variability. This pair exhibits a canonical correlation between the precipitation and the multicomponent field coefficient time series of 0.92. The canonical patterns of the geopotential height fields and SLP (fig. 4a-c) present an equivalent barotropic structure throughout the entire troposphere with strong positive (negative) anomalies centred over northwestern Europe. The central and western Mediterranean lie at the southern margin of this anomaly pattern. A negative (positive) height anomaly centred north of the Caspian Sea covers the Eastern Mediterranean. The corresponding wet season precipitation anomaly pattern (fig. 4d) indicates below (above) normal values almost over the entire basin, except for the southeastern Mediterranean. The last graph of fig. 4 presents the variations of the normalised monthly time components of the first CCA pair. The correlation between the precipitation canonical series and the Mediterranean wet season precipitation is 0.72 (significant at the 95% level). Thus, it seems that there is a relevant contribution from this canonical mode to the long-term trends in wet season Mediterranean precipitation. Wet half year periods are observed in the 1960s, the end of 1970s and single years at the 1980s and 1990s; dry seasons are found during the 1950s, the first part of the 1970s, the end of the 1980s and beginning of the 1990s. Especially the end of the 1980s and early 1990s are well known for general drought conditions over large parts of the Mediterranean [15, 5, 18]. The positive phase of this CCA is associated with negative rainfall anomalies over the western, central and northern Mediterranean area. Wetter conditions prevail over the remaining region. The lowest precipitation anomalies in the CCA1 pattern are prevalent along the western side of the Dynarides and Pindos. An anomalous high-pressure system dominates over the entire Mediterranean at upper levels as well as at sea level. This blocking high obstructs the low-pressure systems of Atlantic origin from crossing the Mediterranean. There, atmospheric stability and subsidence lead to below normal precipitation. Above normal wet season precipitation

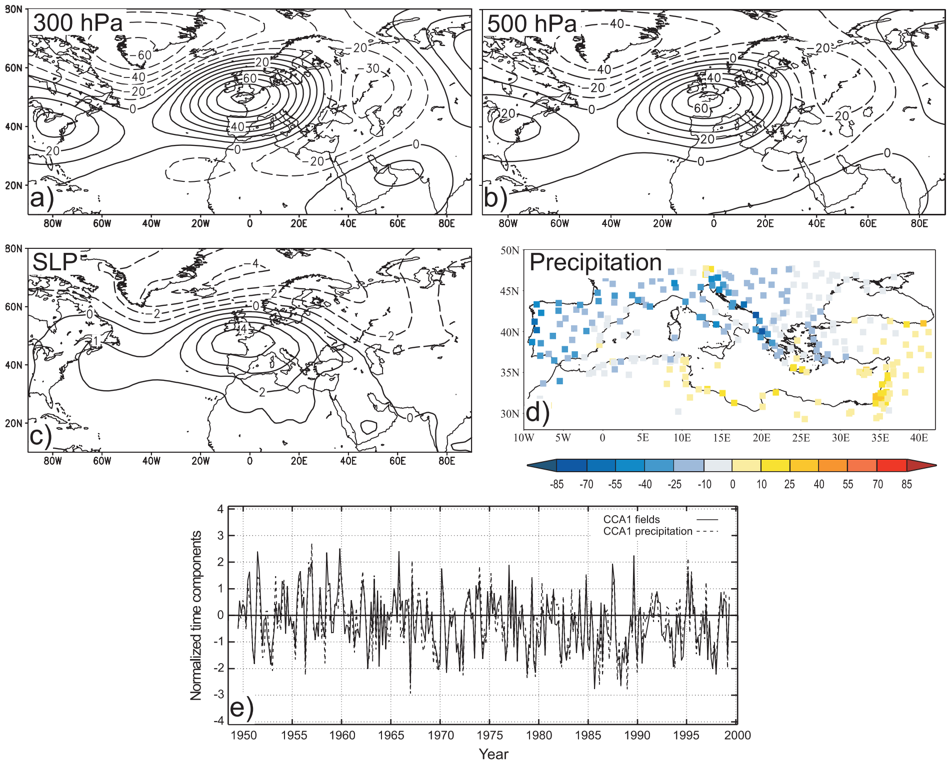


Fig. 4. – Canonical spatial patterns of the first CCA. The canonical correlation patterns reflect the typical strength of the signal, with a) 300 hPa; b) 500 hPa; c) SLP; d) wet season precipitation anomalies in mm; e) normalised time components of CCA1 (from Xoplaki *et al.*, 2004).

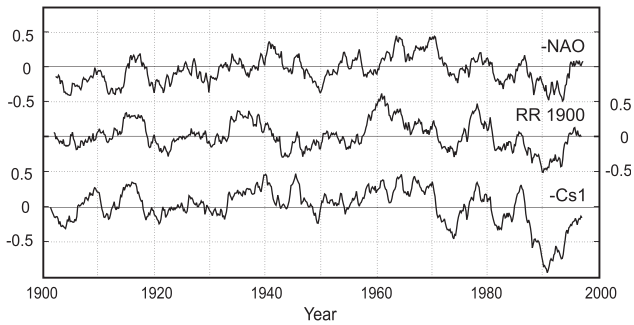


Fig. 5. – −NAO: Gibraltar-Iceland NAO index (Jones *et al.*, 1997) with reversed sign. −Cs1: regressed time series (4-years moving average filter) between the NCAR SLP dataset (Trenberth and Paolino, 1980) and the SLP pattern in fig. 4c with reversed sign.

characterizes the Near East and northern Africa. A negative height anomaly centred north of the Caspian Sea covers the Eastern Mediterranean, bringing cooler air masses of northern origin that cross the warm eastern Mediterranean basin. The connected instability is related to the wetter conditions over the eastern basin.

Concerning decadal and long-term trends, the first two CCA modes seem to have contributed to the low precipitation records in the late 1980s and early 1990s. However, the first mode is more in agreement with changes in spatial precipitation average (not shown) during the period 1949-1999. A natural question is whether the relationships are persistence before the 1950s. In fig. 5 RR 1900 shows standardised averages (4-year moving averages) of all stations with continuous measurements back to 1900. For the first half of the twentieth century RR 1900 indicates the relatively dry (early 1900s, early 1920s and 1940s) and wet periods (1910s and 1930s). It is suggested as well that the decreasing trend highlighted in of the second part of the twentieth century is not part of a longer period trend but a feature of the second half of the twentieth century and that the 1960s and late 1970s were actually the wettest intervals since the 1850s.

Some support for this reasoning can be found in the evolution of the large-scale circulation during the twentieth century shown in fig. 5. Since the NCEP/NCAR reanalysis dataset cannot provide information before the 1950s, the NCAR SLP dataset [26] was used. The time series labelled as Cs1 (fig. 5) shows the regressed time series (4-year moving average filter) between the SLP dataset (1900 to 1999) and the SLP pattern in fig. 4c with reversed sign. Cs1 can be considered as estimation with minimum error of the intensities of the reversed canonical series in fig. 4e through the entire twentieth century using the information provided by the SLP dataset. It becomes quite apparent that −Cs1 and RR 1900 show similar decadal changes since the beginning of the twentieth century (correlation 0.76). For comparison reasons, fig. 5 shows also the Gibraltar-Iceland NAO index [11] with reversed sign (−NAO). The correlation of this time series with −Cs1 is 0.70, suggesting that the long-term changes experienced by the first CCA mode are basically influenced by the NAO. After (before) 1960, both −Cs1 and −NAO show negative (positive) trends supporting the idea that the negative precipitation trends after the 1950s are dynamically induced and a feature of the second half of the twentieth century.

## 4. – Conclusions

In this study, the interannual to decadal connection between the Mediterranean summer (JJAS) surface air temperature and wet season (October-March) precipitation and the state of the large-scale atmospheric circulation, the thickness patterns as well as the Mediterranean SSTs, was investigated for the period 1950-1999. Warmer Mediterranean summers are characterizing the 1950s, 1980s and 1990s and cooler summers were prevalent from the mid-1960s to the mid-1970s. Warm summers are related to blocking conditions, subsidence and stability over the Mediterranean. Further, warm summers can be attributed to a warm lower troposphere as shown by thickness variables and positive Mediterranean SSTs. The summer temperature during the period 1950-1999 increased significantly in western and central Mediterranean but not in the eastern basin. The basic difference in the trends between the eastern and western basins over the last few decades suggests that there is a complex relationship between the Mediterranean climate and the general atmospheric circulation and SSTs. Thus, on a wider scale, the climate variability, changes in the air temperature and precipitation distribution, is influenced by changes in the atmospheric circulation, which in turn alters the storm tracks and the air temperature and precipitation distribution. It has been found that the overall summer warming of around 0.4 °C over the second part of the twentieth century can be mainly attributed to the first Canonical mode, associated with blocking conditions, subsidence, stability and above normal Mediterranean Sea Surface temperatures. On average, the Mediterranean summer temperature from 1500 to 1800 reached values similar to mean twentieth century conditions, though connected with uncertainties of the range of 0.8 °C. The coldest 100-year period was experienced in the nineteenth century. Over the last good 100 years, there were two strong summer warming trends detectable, the later leading to the warmest summers within the last 505 years. The summer of 2003 marks by far the hottest summer exceeding almost 5 standard deviations of the 1901-2000 period. Further work will deal with temperature and precipitation reconstructions for all seasons, spatial maps and associated uncertainties including the most appropriate documentary and natural proxy information from the Mediterranean and its vicinity.

Below normal precipitation over most of the Mediterranean region with lowest values at the western coasts of the peninsulas and highest at the southeastern part of the basin correlates with NAO/AO and EA/WRUS. This expression of the first canonical mode could be interpreted as northward shifts of storm tracks from the Mediterranean towards western and northern Europe that produce the dryness over the Mediterranean.

Although large-scale atmospheric features account for a rather high amount of overall Mediterranean variation, smaller scale processes also influence regional rainfall variability. Land-sea effects and interactions, the influence of the SSTs connected with latent and sensible heat flux, orographical features and thermodynamical aspects interact with each other on different time scales and are superimposed on the quasi-stationary planetary waves which control large-scale advection. The analysis of precipitation trends for the 1949 to 1999 period and back to the beginning of the nineteenth century reveals that wet season precipitation increased in the Mediterranean since the beginning of the period with a maximum in the 1960s and decreased since then. Single wet periods occurred in the late 1970s, early 1980s and late 1990s. The second half of the twentieth century shows a general downward trend of 2.2 mm $\times$ month $-1$ decade $-1$. Especially the end of the 1980s-early 1990s are well known for general drought conditions over the large parts of the Mediterranean. These decadal and long-term trends follow those of the Gibraltar-Iceland NAO, thus results suggest that long-term changes in Atlantic variability govern Mediterranean precipitation. Additionally, the downward trend of the last decades of the twentieth century does not belong to a longer period trend.

## REFERENCES

[1] Barnett T. P. and Preisendorfer R. W., *Mon. Weather Rev.*, **115** (1987) 1825.

[2] Brunet M., Aguilar E., Saladie O., Sigró J. and López D., in *Detecting and Modelling Regional Climate Change*, edited by Brunet M. and López D. (Springer Verlag, Berlin, Heidelberg, New York) 2001, pp. 81-93.

[3] Brunet M., Aguilar E., Saladie O., Sigró J. and López D., in *13th Symposium on Global change and Climate Variations, Orlando 2002* (American Meteorological Society, Boston) 2002, pp. 30-32.

[4] Edwards A. L., *An Introduction to Linear Regression and Correlation*, 2nd ed. (Freeman W. H., New York) 1984, pp. 81-83.

[5] Eshel G. and Farrell B. F., *J. Atmos. Sci.*, **57** (2000) 3219.

[6] Folland C. K. *et al.*, in Chapter 2 of *Climate change 2001; the scientific basis, Contribution of Working Group I to the Third Assessment Report of the Intergovernmental Panel on Climate Change*, edited by Houghton J. T. *et al.* (Cambridge University Press, Cambridge, UK and New York, NY, USA) 2001.

[7] Galán E., Cañada R., Fernández F. and Cervera B., in *Detecting and modelling regional climate change*, edited by Brunet M. and López D. (Springer Verlag, Berlin, Heidelberg, New York) 2001, pp. 119-131.
[8] Giorgi F., *Clim. Dyn.*, **18** (2001) 675, doi 10.1007/s00382-001-0204-x.
[9] Hansen J., Ruedy R., Sato M., Imhoff M., Lawrence W., Easterling D., Peterson T. and Karl T., *J. Geophys. Res.*, **106** (2001) 23947.
[10] Jacobeit J., *Petermanns Geographische Mitteilungen*, **144** (2000) 22.
[11] Jones P. D., Jonsson T. and Wheeler D., *Int. J. Climatol.*, **17** (1997) 1433.
[12] Jones P. D. and Mann M. E., *Rev. Geophys.*, **42** (2004) RG2002, doi: 10.1029/2003RG000143.
[13] Kalnay E. *et al.*, *Bull. Am. Meteorol. Soc.*, **77** (1996) 437.
[14] Kistler R. *et al.*, *Bull. Am. Meteorol. Soc.*, **82** (2001) 247.
[15] Kutiel H., Maheras P. and Guika S., *Theor. Appl. Climatol.*, **54** (1996) 125.
[16] Livezey R. E. and Smith T. M., *J. Climate*, **12** (1999) 303.
[17] Luterbacher J., Dietrich D., Xoplaki E., Grosjean M. and Wanner H., *Science*, **303** (2004) 1499.
[18] Maheras P., in *Drought and Drought Mitigation in Europe*, edited by Vogt J. V. and Somma F. (Kluwer Academic Publishers) 2000, pp. 91-102.
[19] Michaelsen J., *J. Clim. Appl. Meteorol.*, Vol. **26** (1987) 1589.
[20] North G. R., Moeng F. J., Bell T. L. and Cahalan R. F., *Mon. Weather Rev.*, **110** (1982) 319.
[21] New M. G., Hulme M. and Jones P. D., *J. Climate*, **13** (2000) 2217.
[22] New M., Todd M., Hulme M. and Jones P. D., *Int. J. Climatol.*, **21** (2001) 1899.
[23] Peterson T. C. ans Vose R. S., *Bull. Am. Meteorol. Soc.*, **78** (1997) 2837.
[24] Peterson T. C., Vose R. S., Schmoyer R. and Razuvaëv V., *Int. J. Climatol.*, **18** (1998) 1169.
[25] Rayner N. A., Horton E. B., Parker D. E., Folland C. K. and Hackett R. B., Version 2.2 of the Global Sea-Ice and Sea Surface Temperature Data Set, 1903-1994, *Climate Research Technical Note 74*, unpublished document available from Hadley Centre (1996).
[26] Trenberth K. and Paolino D. A., *Mon. Weather Rev.*, **108** (1980) 855.
[27] Türkeş M., *Int. J. Climatol.*, **16** (1996) 1057.
[28] Türkeş M., *Int. J. Climatol.*, **18** (1998) 649.
[29] Von Storch H. and Zwiers F. W., *Statistical Analysis in Climate Research* (Cambridge University Press, UK) 1999.
[30] Vose R. S., Schmoyer R. L., Steurer P. M., Peterson T. C., Heim R., Karl T. R. and Eischeid J., The Global Historical Climatology Network: long-term monthly temperature, precipitation, sea level pressure, and station pressure data, ORNL/CDIAC-53, NDP- 041, Carbon Dioxide Information Analysis Center, Oak Ridge National Laboratory, Oak Ridge, Tennessee (1992).
[31] Wilks D. S., in *Statistical Methods in the Atmospheric Sciences: An Introduction*, edited by Dmowska R. and Holton J. R., *International Geophysics Series*, Vol. **59** (Academic Press) 1995.
[32] Xoplaki E., *Climate Variability in the Mediterranean*, Ph.D. Thesis, University of Bern (2002), p. 193.
[33] Xoplaki E., González-Rouco J. F., Gyalistras D., Luterbacher J., Rickli R. and Wanner H., *Clim. Dyn.*, **20** (2003) 523.
[34] Xoplaki E., González-Rouco J. F., Luterbacher J. and Wanner H., *Clim. Dyn.*, **20** (2003) 723.
[35] Xoplaki E., González-Rouco J. F., Luterbacher J. and Wanner H., *Clim. Dyn.*, **23** (2004) 63.
[36] Xoplaki E., Luterbacher J., Paeth H., Dietrich D., Steiner N., Grosjean M. and Wanner H., *Geophys. Res. Lett.*, **32** (2005) L15713.